Lawrence Berkeley National Laboratory

Title
Understanding the crack formation of graphite particles in cycled commercial lithium-ion batteries by focused ion beam - scanning electron microscopy

Permalink
https://escholarship.org/uc/item/1d93t5j0

Authors
Lin, Na
Jia, Zhe
Wang, Zhihui
et al.

Peer reviewed

Understanding the crack formation of graphite electrode in cycled commercial lithium-ion batteries by Focused ion beam scanning electron microscopy

Na Lin[1,2], Zhe Jia[1], Zhihui Wang[1], Hui Zhao[1], Guo Ai[1, 5], Xiangyun Song[1], Ying Bai[1,3], Vincent Battaglia[1,] Chengdong Sun[4], Juan Qiao[2], Kai Wu[4] and Gao Liu[1, *]

[1]Energy Technologies Area, Lawrence Berkeley National Laboratory, Berkeley, CA 94720, USA

[2]Department of Chemistry, Tsinghua University, Beijing 100084, China

[3]School of Chemical Engineering & Environment, Beijing Institute of Technology, Beijing, 100081, China

[4]Research Institute, Ningde Amperex Technology Co. Ltd, Ningde, Fujian, China

[5]Science and Technology on Reliability Physics and Application of Electronic Component Laboratory, No.5 Electronic Research Institute of the Ministry of Industry and Information Technology, Guangzhou, China, 510610

[*]Corresponding author, Phone: +1(510) 486-7207, Fax: +1(510) 486-7303, E-mail: gliu@lbl.gov

Abstract

The structure degradation of commercial Lithium-ion battery (LIB) graphite anodes with different cycling numbers and charge rates was investigated by focused ion beam (FIB) and scanning electron microscopy (SEM). The cross-section image of graphite anode by FIB milling shows that cracks, resulted in the volume expansion of graphite electrode during long-term cycling, were formed in parallel with the current collector. The crack occurs in the bulk of graphite particles near the lithium insertion surface, which might derive from the stress induced during lithiation and de-lithiation cycles. Subsequently, crack takes place along grain boundaries of the polycrystalline graphite, but only in the direction parallel with the current collector. Furthermore, fast charge graphite electrodes are more prone to form cracks since the tensile strength of graphite is more likely to be surpassed at higher charge rates. Therefore, for LIBs long-term or high charge rate applications, the tensile strength of

graphite anode should be taken into account.

Key Words: LIB, graphite, FIB, SEM, crack formation

1. Introduction

Today one of the greatest challenges of modern society is to stabilize a consistent energy supply that will meet the growing energy demands. This demand has expanded beyond energy density to include the need for power density as applications such as hybrid/full electric vehicles, and aircraft backup power. Due to the high energy and power density of Li-ion batteries (LIBs), it has become a promising candidate for these portable devices.[1-5] Increasing efforts have been made to investigate the electrode materials to achieve LIBs with good performance, low cost, and safety.

Various anode materials, including graphite, nitrides, tin oxides and tin-based alloys and cathode materials such as $LiCoO_2$, $LiMn_2O_4$, $LiNi_xMn_yCo_{1-x-y}O_2$, $LiNi_xCo_yAl_{1-x-y}O_2$ and $LiFePO_4$ have been studied.[3, 5-11] Among these candidates, Graphite-$LiFeO_4$ is one of the most widely used systems of commercial LIBs, owing to its superb safety feature and prolonged cycle life.[12-14] The long-term failure and degradation mechanism of the Graphite-$LiFeO_4$ batteries are mainly due to the degradation of the graphite anode, although the detailed mechanisms have not been fully identified. To be noted, understanding the degradation mechanisms of LIBs is beneficial to address the life time and safety challenges, to make precise lifetime predictions, and to improve the battery performance.[15] It was found that compared to the stable $LiFeO_4$ electrode,[16] the stability of graphite electrode is more critical to the long-term failure and degradation of the corresponding LIB.[17-20] Therefore, investigating the degradation mechanism of graphite electrodes in Graphite-$LiFeO_4$ batteries would help us understand the decline of battery performance along cycles.

In our previous work, we have studied the stability of graphite particles and PVDF binder in graphite-$LiFeO_4$ batteries and found that the PVDF remain stable but the size of graphite

particle after long-term cycling was ~30% larger than the average size of the particles before cycling, and the d-spacing of the graphene layer distance remains the same before and after cycling. [21] This expansion can hardly be solely explained by the SEI layer growth on the surface of the graphite particles. Thus, in this work, we use the focused ion beam (FIB) and scanning electron microscopy (SEM) to further investigate the origin of the graphite expansion in lithium-ion batteries after long-term cycling. By using the FIB, it is possible to selectively mill material to prepare a series of cross-sectional surfaces of interest, so that we could examine the third dimension of the anode and explore hidden internal microstructure. The microstructure of the graphite anode is further investigated by using the SEM and Transmission Electron Microscope (TEM).

2. Result and discussion

To study the graphite anode volume expansion and the change of the micro and nano structure of the graphite particles, the cells were cycled at 200 and 800 times at 1C. To further investigate the effect of cycling rate, they were also cycled 200 times at different C-rate including 0.5C and 4C at 30 ^{o}C. To ensure that all the cells were fully discharged before they were opened, they were charge-discharged twice after the cycling test. All tested cells were disassembled. The graphite anodes were thoroughly washed by DMC and dried. The micro and nano structure of the graphite anode was investigated by FIB-SEM. A schematic diagram of the geometry of the FIB and SEM columns and typical sample orientation for the serial-sectioning experiment is shown in Figure 1. The standard serial-sectioning procedure for FIB-SEM begins with cross-section FIB milling. FIB is used as a "nano-knife" to slice the electrode materials and to prepare a series of cross-sectional surfaces of the electrode. By investigating the cross-section image of the electrode, the hidden internal micro and nano structure of the material can be revealed.[22, 23] FIB is a relatively gentle process and will be able to preserve the sample integrity as compared to conventional mechanical grinding or polishing methods. Features, such as porosity, crack and comparatively-soft phases, can be well preserved after milling process.[24] Therefore, in this work SEM was employed to analyze the anode internal microstructure after ion milling. The results are presented in Figure 2.
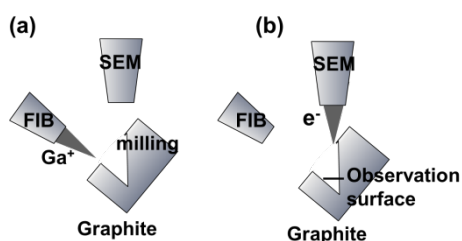
Figure 1. Schematic diagrams of the sample geometry relative to the FIB and SEM columns for serial-sectioning via (a) cross-section milling and (b) SEM imaging.[22]

The cross section areas of both pristine graphite electrode and graphite electrode from anode cycled 200 times at 1C were examined by SEM. As Figure 2(a) shows, the pristine graphite particles before cycling are dense materials with no internal void space. Under SEM, the cross-sections of pristine graphite particles are smooth and free of void space and cracks. After 200 cycles at 1C rate, lots of cracks, being parallel to each other and to the current collector, were observed inside cross section of the cycled graphite particles (Figure 2(b)). The extensive cracks must be formed during the cycling process. We further investigate the effect of the cycling time and cycling number on the crack. As depicted in Figure 2(c), for the graphite particles from the cell cycled 800 times at 1C, cracks could also be observed inside the particles. Furthermore, there are more cracks and significantly larger crack in graphite particles from the cell cycled 800 times compared with those cycled 200 times, indicating the crack size growing with the cycling time and number. Although it is puzzling that the crack only formed in parallel with the current collector and with each other, this is a polymer based laminate pouch cell. The direction perpendicular to the electrode is not subject to large confinement force except the vacuumed pouch confinement. Therefore, cracks on the direct parallel to the current collectors can effectively release the force to the direction perpendicular the current collector, where there is least confinement.
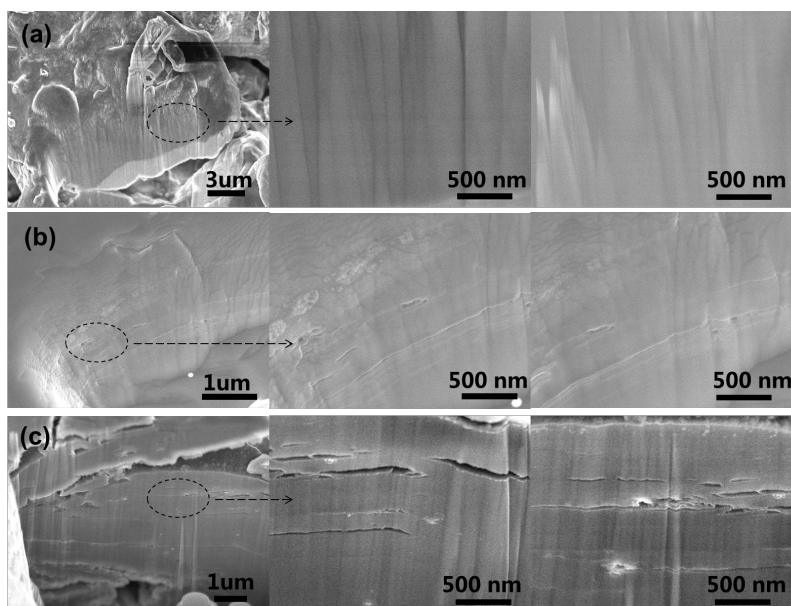
Figure 2. Cross-sectional SEM image of (a) the pristine graphite particles, graphite particles from cells cycled (b) 200 cycles and (c) 800 cycles at 1C.

Furthermore, we employed the low magnification, bright-field TEM to investigate the crystal structure of the graphite particles. Figure 3(a) and (b) are the bright-field TEM image and selected area electron diffraction (SAED) pattern obtained from the pristine graphite particles, respectively. It shows a characteristic polycrystalline diffraction pattern of graphite particles, with d-spacing of 0.34 nm and 0.17 nm, corresponding to the (002) and (004) graphite planes, respectively. In addition, diffraction ring patterns were obtained from (100) (d-spacing=0.20 nm) family of planes, again typical graphite planes. It demonstrates that this graphite particle is a randomly ordered polycrystalline graphitic carbon with a well-defined layered structure.
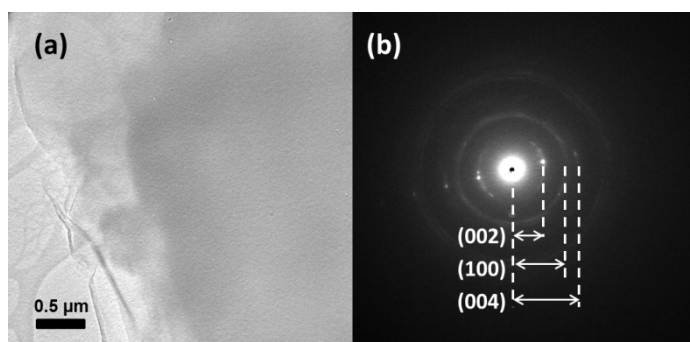

Figure 3. (a) A low magnification, bright-field TEM image of the pristine graphite particle. (b) The SAED pattern obtained from the pristine graphite.

It is reported that the stress generation arising from the lithium insertion into carbon anode[25] or cathodic lattices such as $LiCoO_2$,[25] $LiMn_2O_4$ [26] would produce cracks or fractures in the material. Thus, the stress generated during long-term lithiation/de-lithiation would likewise lead to structure degradation of the graphite anodes in this system at both micro- and nano-scale levels. Noted that the micron size graphite particles are polycrystalline materials, and are randomly distributed in the electrode, it can be deduced that the cracks are likely happening along the grain boundaries of the polycrystalline graphite, which might be derived from the stress induced during the lithiation and de-lithiation process, as illustrated in Figure 4. Upon long-term cycling, cracks propagate along the grain boundaries of the polycrystalline graphite with least resistance, which would result in the volume expansion of the graphite electrode reported previously.[21] As we described in the previous report, no crack observed on the surface of these graphite particles due to the SEI formation, which masks the micro crack on the surface. [21]
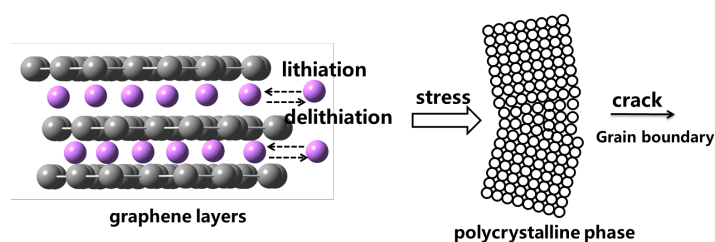

Figure 4. Illustration of the crack formation of the graphite particles from the cycling cells.

The crack formation and propagation also highly depends on the cycling rate (or current density). We further investigate the crack formation inside the graphite particles from cells cycled at different charge and discharge rates. Figure 5 shows the SEM images of the cross-section of graphite particles from cells cycled 200 times at 0.5C (Figure 5a) and 4C (Figure 5b), respectively. Compared to the graphite particles from cell cycled at 1C, cell cycled at 0.5C has very few cracks and much smaller cracks formed inside the particles. In contrast, there are many cracks inside the graphite particles at 4C compared to the graphite at 0.5C rate 200 cycles and 1C rate 800 cycles. However, the cracks are smaller that of the 1C rate 800 cycles. Thus, it can be concluded that the crack initiation sites and crack size of the graphite particles increase with the cycling rate. The crack size is also depending on the cycling time and numbers. Cycling the LIBs at higher rate (higher current density) induces

higher mechanical strain on the graphite lattice of the anode electrode due to the steep gradient of lithium ions.[19, 27] Therefore, the tensile strength of polycrystalline graphite is likely to be surpassed at higher cycling rate, which means crack is prone to form under high current through the electrode. In general, when the crack formed internally in the graphite particles, the surface area of the graphite particle increases gradually even in the high rate (high current) scenario, the elasticity of the SEI layer could accommodate the surface area increase along with the gradual additional SEI formation. However, when the cracks formed on the surface of the graphite particles, new SEI needs to form immediately to stabilize the new crack surface. Both scenarios cause continues electrolyte consumptions, leading to lithium loss and electrolyte starvation, a leading form of cell failure in graphite-LFP batteries.

These findings are significant toward the application of graphite based battery design. First, in the designing of hybrid electric vehicles (HEV), the battery capacity is relatively small. Usually, a current pulse rate of at least 7C is required for the HEV application. This will induce significant graphite anode based degradation due to the graphite cracks discussed here. A relatively large over capacity of the battery maybe needed for improved cycle life performance. Fast charging at 10C rate, eg. 5 minutes to full capacity, is a very desirable properties of the battery at its current energy density, however, graphite may not be the right choice for anode for this application due to the possible poetization of graphite particles.   .
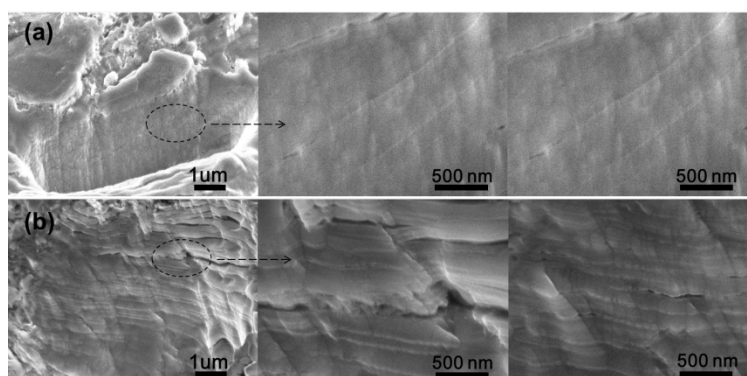

Figure 5. Cross-sectional SEM image of graphite particles from cells with 200 cycles with difference cycling rate: (a) 0.5C and (b) 4C.

3. Conclusion

In summary, the mechanism of structure degradation in commercial graphite electrode was investigated by electron spectroscopy methods. Commercial graphite/LiFePO$_4$ batteries were cycled at different cycling condition (i.e. cycle number and charge/discharge rate). The cycled cells were analyzed by FIB, SEM and TEM. It was found that cracks were initiated and propagated due to the stress induced during lithiation and de-lithiation process. Subsequently, cracks take place along grain boundaries of the polycrystalline graphite. These micro-cracks grow during long-term cycling, which are resulted owing to the volume expansion of the graphite particle, and hence expansion of the overall cell volume. The crack formation sites and the crack size are related to the cycling rate (current density), whereas cycled at high charge rate is prone to have more crack initiation since the tensile strength of graphite is more liable to be surpassed at high charge rates. Thus for the long-term or high charge rate application, the tensile strength of graphite anode should be taken into account.

4. Experiment

4.1 Preparation of graphite anode for FIB/SEM test

The graphite anode samples studied are got from the commercial polymer punch cells which consist of LFP cathode and PVDF binder. The designed capacity of each cell is 1 Ah. The cells were customer fabricated by ATL Co. The graphite anode material were analyzed and documented before they were used. The formation of these cells was done before sending to Lawrence Berkeley National Laboratory for testing and analyses. The galvanostatic charge-discharge tests were performed on those cells using Maccor 4000 at 30 °C between 3V and 4V and different C-rate. Some cells were cycled for 200 times at 0.5C, 1C, or 4C, and some cells were cycled for 200 or 800 times at 1C-rate. One cells was fully charged and periodically recharged to maintain the fully charge state at the time other cells are being cycled. At last, all the cells were charged and discharged 2 times at 0.1C and stopped at discharged state for material harvesting and analyses. Before FIB-SEM testament, all the cells were disassembled in glove box filled with argon. The anodes were washed with DMC thoroughly and dried in the glove box at room temperature. The resulted graphite anode samples were then used for the FIB-SEM test.

4.2 FIB and SEM tests

The cross sectional images of the samples were obtained using a combination of a field-emission scanning electron microscopy with a focused gallium ion beam milling system (FEI Quanta 3D Dual Beam FEG FIB-SEM). Using a 5 nA Ga-ion beam current, a first coarse cross-section was milled as a viewing channel for SEM observation. The exposed surface of this cross-section was fine polished by lowering the ion beam current down to 1.1 nA. Subsequently, the cross-section images were obtained at a 5 kV acceleration potential using the field-emission SEM.

REFERENCES

[1] V. Etacheri, R. Marom, R. Elazari, G. Salitra, D. Aurbach, Challenges in the development of advanced Li-ion batteries: a review, Energ. Environ. Sci., 4 (2011) 3243.

[2] R. Marom, S.F. Amalraj, N. Leifer, D. Jacob, D. Aurbach, A review of advanced and practical lithium battery materials, J. Mater. Chem., 21 (2011) 9938.

[3] N. Nitta, F. Wu, J.T. Lee, G. Yushin, Li-ion battery materials: present and future, Mater. Today, 18 (2015) 252-264.

[4] M.A. Rahman, Y.C. Wong, G. Song, C. Wen, A review on porous negative electrodes for high performance lithium-ion batteries, J. Porous Mater., 22 (2015) 1313-1343.

[5] F. Yao, D.T. Pham, Y.H. Lee, Carbon-Based Materials for Lithium-Ion Batteries, Electrochemical Capacitors, and Their Hybrid Devices, Chem. Sus. Chem., 8 (2015) 2284-2311.

[6] M.A. J.-M. Tarascon, Issues and challenges facing rechargeable lithium batteries, Nature, 414 (2001) 359-367.

[7] V.S. M. Noel, Role of carbon host lattices in Li-ion intercalation/de-intercalation processes, J. Power Sources, 111 (2002) 193-209.

[8] Y.P. Wu, E. Rahm, R. Holze, Carbon anode materials for lithium ion batteries, J. Power Sources, 114 (2003) 228-236.

[9] J. Xu, H.R. Thomas, R.W. Francis, K.R. Lum, J. Wang, B. Liang, A review of processes and technologies for the recycling of lithium-ion secondary batteries, J. Power Sources, 177 (2008) 512-527.

[10] J.W. Fergus, Recent developments in cathode materials for lithium ion batteries, J. Power Sources, 195 (2010) 939-954.

[11] B. Scrosati, J. Garche, Lithium batteries: Status, prospects and future, J. Power Sources, 195 (2010) 2419-2430.

[12] M. Safari, C. Delacourt, Modeling of a Commercial Graphite/LiFePO4 Cell, J. Electrochem. Soc., 158 (2011) A562.

[13] M. Safari, C. Delacourt, Aging of a Commercial Graphite/LiFePO4 Cell, J. Electrochem. Soc., 158 (2011) A1123.

[14] H. Song, Z. Cao, X. Chen, H. Lu, M. Jia, Z. Zhang, Y. Lai, J. Li, Y. Liu, Capacity fade of LiFePO4/graphite cell at elevated temperature, J. Solid State Electrochem., 17 (2012) 599-605.

[15] C. Lin, A. Tang, H. Mu, W. Wang, C. Wang, Aging Mechanisms of Electrode Materials in Lithium-Ion Batteries for Electric Vehicles, J. Chem, 2015 (2015) 1-11.

[16] K. Zaghib, K. Striebel, A. Guerfi, J. Shim, M. Armand, M. Gauthier, LiFePO4/polymer/natural graphite: low cost Li-ion batteries, Electrochim. Acta, 50 (2004) 263-270.

[17] E.Z. Doron Aurbach, Yaron Cohen, Hanan Teller, A short review of failure mechanisms of lithium metal and lithiated graphite anodes in liquid electrolyte solutions, Solid State Ionics, 148 (2002) 405-416.

[18] J. Vetter, P. Novák, M.R. Wagner, C. Veit, K.C. Möller, J.O. Besenhard, M. Winter, M. Wohlfahrt-Mehrens, C. Vogler, A. Hammouche, Ageing mechanisms in lithium-ion batteries, J. Power Sources, 147 (2005) 269-281.

[19] V. Agubra, J. Fergus, Lithium Ion Battery Anode Aging Mechanisms, Materials (Basel), 6 (2013) 1310-1325.

[20] A. Barré, B. Deguilhem, S. Grolleau, M. Gérard, F. Suard, D. Riu, A review on lithium-ion battery ageing mechanisms and estimations for automotive applications, J. Power Sources, 241 (2013) 680-689.

[21] K. Dai, Z. Wang, G. Ai, H. Zhao, W. Yuan, X. Song, V. Battaglia, C. Sun, K. Wu, G. Liu, The transformation of graphite electrode materials in lithium-ion batteries after cycling, J. Power Sources, 298 (2015) 349-354.

[22] D.J. Stokes, F. Morrissey, B.H. Lich, A New Approach to Studying Biological and Soft Materials Using Focused Ion Beam Scanning Electron Microscopy (FIB SEM), J. Phys. Conf. Ser., 26 (2006) 50-53.

[23] H. Iwai, N. Shikazono, T. Matsui, H. Teshima, M. Kishimoto, R. Kishida, D. Hayashi, K. Matsuzaki, D. Kanno, M. Saito, H. Muroyama, K. Eguchi, N. Kasagi, H. Yoshida, Quantification of SOFC anode microstructure based on dual beam FIB-SEM technique, J. Power Sources, 195 (2010) 955-961.

[24] M.D. Uchic, M.A. Groeber, D.M. Dimiduk, J.P. Simmons, 3D microstructural characterization of nickel superalloys via serial-sectioning using a dual beam FIB-SEM, Scr. Mater., 55 (2006) 23-28.

[25] S. Renganathan, G. Sikha, S. Santhanagopalan, R.E. White, Theoretical Analysis of Stresses in a Lithium Ion Cell, J. Electrochem. Soc., 157 (2010) A155.

[26] X. Zhang, W. Shyy, A. Marie Sastry, Numerical Simulation of Intercalation-Induced Stress in Li-Ion Battery Electrode Particles, J. Electrochem. Soc., 154 (2007) A910.

[27] J. Christensen, J. Newman, Stress generation and fracture in lithium insertion materials, J. Solid State Electrochem., 10 (2006) 293-319.